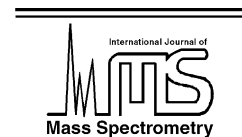




ELSEVIER

International Journal of Mass Spectrometry 228 (2003) 1099–1109



www.elsevier.com/locate/ijms

Subject index Volume 228

Ab initio

- Ab initio characterization of the weakly bound anions ClOO^- and ArCl^- , 667
- Theoretical studies of methane elimination from C_4H_9^+ and H_2 elimination from C_3H_7^+ , 955

Ab initio calculations

- Beryllium–helium cations: computational evidence for a large class of thermodynamically stable species, 415

Absolute cross sections

- Experimental studies on the formation of argon atoms in Ar^+ –atoms collisions, 107

Acetone cations

- Surface-induced dissociation of acetone cations from self-assembled monolayer surface of fluorinated alkyl thiol on Au (1 1 1) substrate at low collision energies, 563

Acetone–water clusters

- Ultrafast dynamics of acetone–water clusters: the influence of solvation, 677

Acetonitrile

- Quantification of acetonitrile in exhaled breath and urinary headspace using selected ion flow tube mass spectrometry, 655
- Atmospheric pressure photoionization mechanisms. 1. The case of acetonitrile, 841

Actinide ions

- FTICR-MS study of the gas-phase thermochemistry of americium oxides, 457

Acylium ions

- Reactions of gaseous halocarbonyl cations with aromatic compounds: ionic carbonylation of inert C–H bonds, 901

Adenine radical

- Neutralization–reionization of ions produced by electrospray. Instrument design and initial data, 687

$\text{Ag}_2^+(\text{O}_2)_n$ cluster

- Bonding interactions in $\text{Ag}^+(\text{O}_2)_n$ and $\text{Ag}_2^+(\text{O}_2)_n$ clusters: experiment and theory, 865

Alkane elimination

- Theoretical studies of methane elimination from C_4H_9^+ and H_2 elimination from C_3H_7^+ , 955

1-Alkenes

- Specific reactivity of 1-alkenes with transition metal cations. 1-Pentene– and 1-octene– Cu^+ reactions in the gas phase, 359

Alzheimer's disease

- Zinc binding properties of the amyloid fragment $\text{A}\beta(1-16)$ studied by electrospray-ionization mass spectrometry, 999

Americium oxides

- FTICR-MS study of the gas-phase thermochemistry of americium oxides, 457

Amino acid clusters

- Structural determinants for the evaporation of intact oligomers from collisionally activated cluster ions, 933

Amino acid radicals

- Neutralization–reionization of ions produced by electrospray. Instrument design and initial data, 687

Amino acids

- Na^+ affinities of gas-phase amino acids by ligand exchange equilibrium, 825

α -Aminophosphonic acids

- Gas-phase basicity and enantiodiscrimination of some phosphorous-containing α -amino acid mimics, 349

Ammonia

- Gas-phase ion chemistry in $\text{GeH}_4/\text{C}_2\text{H}_4/\text{XH}_3$ ($\text{X} = \text{P}, \text{N}$) systems, 403

Amyloid peptide

- Zinc binding properties of the amyloid fragment $\text{A}\beta(1-16)$ studied by electrospray-ionization mass spectrometry, 999

Angular distributions

- Experimental studies on the formation of argon atoms in Ar^+ –atoms collisions, 107

Anion

- The impervious route to the elusive HOOO^- anion, 717

Anionic precursors

- Generation of neutrals from anionic precursors in the gas phase. The anionic, neutral and cationic rearrangements of CCCCHO and CCCHCO to HCCCCO , 467

APPI

- Atmospheric pressure photoionization mechanisms. 1. The case of acetonitrile, 841

AQCC

- A theoretical study of the ground and excited states of the CHCl_2^+ dication and the CHCl^+ cation, 497

Ar

- Experimental studies on the formation of argon atoms in Ar^+ –atoms collisions, 107

Ar^+

- Experimental studies on the formation of argon atoms in Ar^+ –atoms collisions, 107

Argon chloride

- Ab initio characterization of the weakly bound anions ClOO^- and ArCl^- , 667

Aromatic C–H bond activation

Reactions of gaseous halocarbonyl cations with aromatic compounds: ionic carbonylation of inert C–H bonds, 901

Atmospheric chemistry

On gaseous $C_4H_6O_2$ compounds in the atmosphere: new insights from collision experiments of the protonated molecules in the laboratory and on aircraft, 35

Benzenedicarboxylic acid dimethyl ester

On the chemistry following methoxy migration in the metastably decomposing $(M - COOCH_3)^+$ ions (m/z 135) from dimethyl phthalate, isophthalate and terephthalate, 891

Benzophenone photoprobe

Tandem mass spectrometric characterization of branched peptides derived from photoaffinity labeling, 527

Beryllium

Beryllium–helium cations: computational evidence for a large class of thermodynamically stable species, 415

Bicyclo[2.2.2]octanes

Proton-induced intra-complex hydride transfer involving bicyclo[2.2.2]octane units as a rigid spacer and as a carbocation precursor, 321

Bidentate bases

Application of the kinetic method to bifunctional bases. ESI tandem quadrupole experiments, 1035

Binding energies

Determining C_2 binding energies from KERDs for C_{80}^+ and C_{82}^+ fullerenes and their endohedrals, 181

Bond energies

Sequential bond energies of $Ag^+(H_2O)_n$ and $Ag^+(\text{dimethyl ether})_n$, $n = 1-4$, determined by threshold collision-induced dissociation, 221

Bonding

Two-center three-electron bonds involving selenium, 429

Bonding interactions

Bonding interactions in $Ag^+(O_2)_n$ and $Ag_2^+(O_2)_n$ clusters: experiment and theory, 865

Breakdown curves

ESI/MS/MS in characterization of diastereomeric intermediates in the stereocontrolled synthesis of protoberberines, 209

Breath

Quantification of acetonitrile in exhaled breath and urinary headspace using selected ion flow tube mass spectrometry, 655

2-Bromopropene radical cation

Reactions of 2-bromopropene radical cation with amines—a study by FT-ICR spectrometry and DFT calculation, 167

Carbene

Electrospray ionization and liquid secondary ion mass spectrometric study of N-heterocyclic carbenes and their 1,2,4-triazolium salt precursors, 61

Carbene precursors

Electrospray ionization and liquid secondary ion mass spectrometric study of N-heterocyclic carbenes and their 1,2,4-triazolium salt precursors, 61

Carbon cycle

Stable isotope ratio mass spectrometry in global climate change research, 1

Carbon dioxide

Field-induced ionization and Coulomb explosion of CO_2 by intense femtosecond laser pulses, 81

Carbonylation

Reactions of gaseous halocarbonyl cations with aromatic compounds: ionic carbonylation of inert C–H bonds, 901

Carboxylic acids

On gaseous $C_4H_6O_2$ compounds in the atmosphere: new insights from collision experiments of the protonated molecules in the laboratory and on aircraft, 35

Structures and fragmentations of electrosprayed Zn(II) complexes of carboxylic acids in the gas phase. Isomerisation versus desolvation during the last desolvation step, 779

Catalysis

Catalytic gas phase dehydration of acetic acid to ketene, 599

Catenanes

Distinguishing the topology of macrocyclic compounds and catenanes, 373

Cations

Specific reactivity of 1-alkenes with transition metal cations. 1-Pentene– and 1-octene– Cu^+ reactions in the gas phase, 359

CBS-QB3 model chemistry

The remarkable decarbonylation of $CH_3O-P=O^+$ and its distonic isomer $CH_2O-P-OH^+$: an experimental and CBS-QB3 computational study, 759

 $C_4F_4Cl_2$ (1,2-dichlorotetrafluorocyclobutene)

Electron attachment and detachment: cyclo- $C_4F_4Cl_2$, 541

 CH_4

Cross sections and ion kinetic energies for electron impact ionization of CH_4 , 307

 $C_3H_7^+$

Theoretical studies of methane elimination from $C_4H_9^+$ and H_2 elimination from $C_3H_7^+$, 955

 $C_4H_9^+$

Theoretical studies of methane elimination from $C_4H_9^+$ and H_2 elimination from $C_3H_7^+$, 955

 $C_4H_4^+$ ion

How ergodic is the fragmentation of the pyridine cation? A maximum entropy analysis, 389

Charge solvated

Investigations of the gas-phase reactivity of Cu^+ and Ag^+ glycine complexes towards CO, D_2O and NH_3 , 629

Charge transfer

Experimental studies on the formation of argon atoms in Ar^+ –atoms collisions, 107

Selected ion flow tube, SIFT, studies of the reactions of H_3O^+ , NO^+ and O_2^+ with eleven $C_{10}H_{16}$ monoterpenes, 117

Reactions of molecular dications: collision energy dependence of integral cross-sections of processes in $CHCl_2^{2+} + Ar$, D_2 systems from guided beam studies, 487

Ion/ion reactions of multiply charged nucleic acid anions: electron transfer, proton transfer, and ion attachment, 577

Chemical ionization (CI)

On gaseous $C_4H_6O_2$ compounds in the atmosphere: new insights from collision experiments of the protonated molecules in the laboratory and on aircraft, 35

Protonation and methylation of thiophenol, thioanisole and their halogenated derivatives: mass spectrometric and computational study, 151

The role of hydride migration in the mechanism of alcohol elimination from protonated ethers upon chemical ionization. Experiment and theory, 297

Fragmentations of some dinitrile anions, 1083

Chemical mass shift

Theory, simulation and measurement of chemical mass shifts in RF quadrupole ion traps, 237

Chlorinated fullerenes

The influence of phenylated by-products on the MALDI analysis of chlorinated fullerenes, 979

Chlorine dioxide

Ab initio characterization of the weakly bound anions $ClOO^-$ and $ArCl^-$, 667

 $C_4H_6O_2$

On gaseous $C_4H_6O_2$ compounds in the atmosphere: new insights from collision experiments of the protonated molecules in the laboratory and on aircraft, 35

 CH_3O migration

On the chemistry following methoxy migration in the metastably decomposing $(M - COOCH_3)^+$ ions (m/z 135) from dimethyl phthalate, isophthalate and terephthalate, 891

 CH_3PO_2 isomers

The remarkable decarbonylation of $CH_3O-P=O^{*+}$ and its distonic isomer $CH_2O-P-OH^{*+}$: an experimental and CBS-QB3 computational study, 759

Citraconates

The distinctive behavior of isomeric methyl ethyl mixed esters of 2-methylmaleic acid upon electron ionization, 191

Climate change

Stable isotope ratio mass spectrometry in global climate change research, 1

Cluster evaporation

Structural determinants for the evaporation of intact oligomers from collisionally activated cluster ions, 933

Clusters

Ultrafast dynamics of acetone–water clusters: the influence of solvation, 677

Structural determinants for the evaporation of intact oligomers from collisionally activated cluster ions, 933

 CO_2^{2+}

Internal energy effects in the reactivity of CO_2^{2+} doubly charged molecular ions with CO_2 and CO , 507

Collisional activation

Protonation and methylation of thiophenol, thioanisole and their halogenated derivatives: mass spectrometric and computational study, 151

Collision-induced dissociation (CID)

On gaseous $C_4H_6O_2$ compounds in the atmosphere: new insights from collision experiments of the protonated molecules in the laboratory and on aircraft, 35

The distinctive behavior of isomeric methyl ethyl mixed esters of 2-methylmaleic acid upon electron ionization, 191

Tandem mass spectrometric characterization of branched peptides derived from photoaffinity labeling, 527

Collision-induced symmetric fission of doubly-charged cubelike $[Fe_4S_4X_4]^{2-}$ clusters, 797

Computation

Microsolvation of metal ions: on the stability of $[Zr(CH_3CN)]^{4+}$ and other multiply charged ions, 517

Concerted elimination

Theoretical studies of methane elimination from $C_4H_9^+$ and H_2 elimination from $C_3H_7^+$, 955

Corticotropin-releasing factor (CRF)

Tandem mass spectrometric characterization of branched peptides derived from photoaffinity labeling, 527

Coulomb explosion

Field-induced ionization and Coulomb explosion of CO_2 by intense femtosecond laser pulses, 81

Coulomb repulsion

Electron affinity versus Coulomb repulsion—when dialkoxides become stable gas phase species, 341

Cross sections

Cross sections and ion kinetic energies for electron impact ionization of CH_4 , 307

2D gels

Structural identification and quantification of protein phosphorylations after gel electrophoretic separation using Fourier transform ion cyclotron resonance mass spectrometry and laser ablation inductively coupled plasma mass spectrometry, 985

Decarbonylation

The remarkable decarbonylation of $CH_3O-P=O^{*+}$ and its distonic isomer $CH_2O-P-OH^{*+}$: an experimental and CBS-QB3 computational study, 759

Density functional calculations

The role of hydride migration in the mechanism of alcohol elimination from protonated ethers upon chemical ionization. Experiment and theory, 297

Density functional theory

On gaseous $C_4H_6O_2$ compounds in the atmosphere: new insights from collision experiments of the protonated molecules in the laboratory and on aircraft, 35

Electron attachment and detachment: cyclo- $C_4F_4Cl_2$, 541

Density functional theory calculations

Specific reactivity of 1-alkenes with transition metal cations. 1-Pentene- and 1-octene- Cu^+ reactions in the gas phase, 359

Desolvation

Structures and fragmentations of electrosprayed $Zn(II)$ complexes of carboxylic acids in the gas phase. Isomerisation versus desolvation during the last desolvation step, 779

Desorbed species

Intermediate species in a 2.45 GHz microwave plasma sustained in an argon–tetramethylsilane gas mixture, 49

Deuterium labeling

The distinctive behavior of isomeric methyl ethyl mixed esters of 2-methylmaleic acid upon electron ionization, 191

- DFT**
Reactions of 2-bromopropene radical cation with amines—a study by FT-ICR spectrometry and DFT calculation, 167
- DFT calculations**
The distinctive behavior of isomeric methyl ethyl mixed esters of 2-methylmaleic acid upon electron ionization, 191
- Dianions**
Electron affinity versus Coulomb repulsion—when dialkoxides become stable gas phase species, 341
- Diastereoisomers**
ESI/MS/MS in characterization of diastereomeric intermediates in the stereocontrolled synthesis of protoberberines, 209
- Dication**
Reactions of molecular dications: collision energy dependence of integral cross-sections of processes in $\text{CHCl}_2^{2+} + \text{Ar}$, D_2 systems from guided beam studies, 487
A theoretical study of the ground and excited states of the CHCl_2^{2+} dication and the CHCl^+ cation, 497
Internal energy effects in the reactivity of CO_2^{2+} doubly charged molecular ions with CO_2 and CO , 507
- Dimethyl ether**
Sequential bond energies of $\text{Ag}^+(\text{H}_2\text{O})_n$ and $\text{Ag}^+(\text{dimethyl ether})_n$, $n = 1-4$, determined by threshold collision-induced dissociation, 221
- Dimolybdate**
Catalytic gas phase dehydration of acetic acid to ketene, 599
- Discharge plasma**
Optical detection of C_9H_3 , C_{11}H_3 , and C_{13}H_3 from a hydrocarbon discharge source, 647
- Dissociative electron attachment**
Formation of negative ions from gas phase halo-uracils by low-energy (0–18 eV) electron impact, 703
- ECD**
Secondary fragmentation of linear peptides in electron capture dissociation, 723
- Electron affinity**
Electron affinity versus Coulomb repulsion—when dialkoxides become stable gas phase species, 341
Electron attachment and detachment: cyclo- $\text{C}_4\text{F}_4\text{Cl}_2$, 541
Ab initio characterization of the weakly bound anions ClOO^- and ArCl^- , 667
Formation of negative ions from gas phase halo-uracils by low-energy (0–18 eV) electron impact, 703
- Electron attachment**
Electron attachment and detachment: cyclo- $\text{C}_4\text{F}_4\text{Cl}_2$, 541
- Electron capture dissociation**
Secondary fragmentation of linear peptides in electron capture dissociation, 723
- Electron detachment**
Hydration of cyclic oxocarbon dianions, such as $\text{c-C}_5\text{O}_5^{2-}$, in the gas phase. Charge reduction of hydrates by electron detachment or proton transfer. Energy barriers for electron detachment and electron transfer, 1017
- Electron impact ionization**
Cross sections and ion kinetic energies for electron impact ionization of CH_4 , 307
- Electron ionization (EI)**
The distinctive behavior of isomeric methyl ethyl mixed esters of 2-methylmaleic acid upon electron ionization, 191
- Electron transfer**
Reactions of 2-bromopropene radical cation with amines—a study by FT-ICR spectrometry and DFT calculation, 167
- Electronic spectroscopy**
Optical detection of C_9H_3 , C_{11}H_3 , and C_{13}H_3 from a hydrocarbon discharge source, 647
- Electrospray**
Hydrogen/deuterium exchange of electrosprayed ions in the atmospheric interface of a commercial triple-quadrupole mass spectrometer, 729
Structures and fragmentations of electrosprayed Zn(II) complexes of carboxylic acids in the gas phase. Isomerisation versus desolvation during the last desolvation step, 779
Collision-induced symmetric fission of doubly-charged cubelike $[\text{Fe}_4\text{S}_4\text{X}_4]^{2-}$ clusters, 797
- Electrospray interface**
Neutralization–reionization of ions produced by electrospray. Instrument design and initial data, 687
- Electrospray ionization**
ESI/MS/MS in characterization of diastereomeric intermediates in the stereocontrolled synthesis of protoberberines, 209
Ion chemistry of the hexanuclear methoxo-oxovanadium cluster $\text{V}_6\text{O}_7(\text{OCH}_3)_{12}$, 743
- Electrospray-ionization mass spectrometry**
Zinc binding properties of the amyloid fragment $\text{A}\beta(1-16)$ studied by electrospray-ionization mass spectrometry, 999
- Eley–Rideal reactions**
Implanting atomic ions into surface adsorbed fullerenes: the single collision formation and emission of Cs@C_{60}^+ and Cs@C_{70}^+ , 1055
- Endohedral fullerenes**
Determining C_2 binding energies from KERDs for C_{80}^+ and C_{82}^+ fullerenes and their endohedrals, 181
Implanting atomic ions into surface adsorbed fullerenes: the single collision formation and emission of Cs@C_{60}^+ and Cs@C_{70}^+ , 1055
- Energy transfer**
Surface-induced dissociation of acetone cations from self-assembled monolayer surface of fluorinated alkyl thiol on Au (1 1 1) substrate at low collision energies, 563
- Enthalpy of formation**
A comprehensive computational investigation of the enthalpies of formation and proton affinities of $\text{C}_4\text{H}_7\text{N}$ and $\text{C}_3\text{H}_3\text{ON}$ compounds, 91
The remarkable decarbonylation of $\text{CH}_3\text{O-P=O}^{\bullet+}$ and its dicationic isomer $\text{CH}_2\text{O-P-OH}^{\bullet+}$: an experimental and CBS-QB3 computational study, 759
- Equilibrium**
Two-center three-electron bonds involving selenium, 429
 Na^+ affinities of gas-phase amino acids by ligand exchange equilibrium, 825
- Esters**
The distinctive behavior of isomeric methyl ethyl mixed esters of 2-methylmaleic acid upon electron ionization, 191

- Ethene
Gas-phase ion chemistry in $\text{GeH}_4/\text{C}_2\text{H}_4/\text{XH}_3$ ($\text{X} = \text{P}, \text{N}$) systems, 403
- Ethers
The role of hydride migration in the mechanism of alcohol elimination from protonated ethers upon chemical ionization. Experiment and theory, 297
- Fast atom bombardement
Fragmentations of some dinitrile anions, 1083
- Femtochemistry
Ultrafast dynamics of acetone–water clusters: the influence of solvation, 677
- Femtosecond
Field-induced ionization and Coulomb explosion of CO_2 by intense femtosecond laser pulses, 81
- Field ionization
Field-induced ionization and Coulomb explosion of CO_2 by intense femtosecond laser pulses, 81
- Finite Heat Bath Theory (FHBT)
Determining C_2 binding energies from KERDs for C_{80}^+ and C_{82}^+ fullerenes and their endohedrals, 181
- Flowing-afterglow Langmuir-probe
Electron attachment and detachment: cyclo- $\text{C}_4\text{F}_4\text{Cl}_2$, 541
- Fluorination
In situ synthesis and characterization of fullerene derivatives by Knudsen-cell mass spectrometry, 807
- Fragmentation mechanisms
Structural analysis of high affinity divalent phosphopeptide hybrids of spleen tyrosine kinase, 879
- Fragmentation pathway
Electrospray ionization and liquid secondary ion mass spectrometric study of N-heterocyclic carbenes and their 1,2,4-triazolium salt precursors, 61
- FT-ICR
Reactions of 2-bromopropene radical cation with amines—a study by FT-ICR spectrometry and DFT calculation, 167
Structure, thermochemistry, and reactivity of MS_n^+ cations ($\text{M} = \text{V}, \text{Mo}; n = 1\text{--}3$) in the gas phase, 439
Secondary fragmentation of linear peptides in electron capture dissociation, 723
 Na^+ affinities of gas-phase amino acids by ligand exchange equilibrium, 825
- FT-ICR-MS
Structural identification and quantification of protein phosphorylations after gel electrophoretic separation using Fourier transform ion cyclotron resonance mass spectrometry and laser ablation inductively coupled plasma mass spectrometry, 985
- FT-MS
Secondary fragmentation of linear peptides in electron capture dissociation, 723
- Fullerenes
Determining C_2 binding energies from KERDs for C_{80}^+ and C_{82}^+ fullerenes and their endohedrals, 181
In situ synthesis and characterization of fullerene derivatives by Knudsen-cell mass spectrometry, 807
Production of small binary carbon clusters by laser ablation of thin films of derivatised fullerenes, 969
- G3 theory
Beryllium–helium cations: computational evidence for a large class of thermodynamically stable species, 415
- G3(MP2)
Electron attachment and detachment: cyclo- $\text{C}_4\text{F}_4\text{Cl}_2$, 541
- Gas phase
Generation of neutrals from anionic precursors in the gas phase. The anionic, neutral and cationic rearrangements of CCCCHO and CCCHCO to HCCCCO , 467
Catalytic gas phase dehydration of acetic acid to ketene, 599
- Gas phase basicity
Application of the kinetic method to bifunctional bases. ESI tandem quadrupole experiments, 1035
- Gas phase ion chemistry
Reactivity of gaseous protonated ozone: a computational investigation on the carbon monoxide oxidation reaction, 613
- Gas-phase enantioselectivity
Gas-phase basicity and enantiodiscrimination of some phosphorous-containing α -amino acid mimics, 349
- Germane
Gas-phase ion chemistry in $\text{GeH}_4/\text{C}_2\text{H}_4/\text{XH}_3$ ($\text{X} = \text{P}, \text{N}$) systems, 403
- Germyl ions
Ligand exchange ion–molecule reactions of simple silyl and germyl cations, 551
- GIB
Structure, thermochemistry, and reactivity of MS_n^+ cations ($\text{M} = \text{V}, \text{Mo}; n = 1\text{--}3$) in the gas phase, 439
- Glycine
Investigations of the gas-phase reactivity of Cu^+ and Ag^+ glycine complexes towards CO , D_2O and NH_3 , 629
- Ground and excited states
A theoretical study of the ground and excited states of the CHCl_2^+ dication and the CHCl^+ cation, 497
- Guided ion beams
Sequential bond energies of $\text{Ag}^+(\text{H}_2\text{O})_n$ and $\text{Ag}^+(\text{dimethyl ether})_n$, $n = 1\text{--}4$, determined by threshold collision-induced dissociation, 221
- H/D exchange
Hydrogen/deuterium exchange of electrosprayed ions in the atmospheric interface of a commercial triple–quadrupole mass spectrometer, 729
- Halocarbonyl cations
Reactions of gaseous halocarbonyl cations with aromatic compounds: ionic carbonylation of inert C–H bonds, 901
- Halo-uracils
Formation of negative ions from gas phase halo-uracils by low-energy (0–18 eV) electron impact, 703
- Helium cations
Beryllium–helium cations: computational evidence for a large class of thermodynamically stable species, 415

- Heterocyclic radicals
Neutralization–reionization of ions produced by electrospray.
Instrument design and initial data, 687
- High-purity material
State-of-the-art in inorganic mass spectrometry for analysis of high-purity materials, 127
- Hydration
Hydration of cyclic oxocarbon dianions, such as $c\text{-C}_5\text{O}_5^{2-}$, in the gas phase. Charge reduction of hydrates by electron detachment or proton transfer. Energy barriers for electron detachment and electron transfer, 1017
- Hydride transfer
Proton-induced intra-complex hydride transfer involving bicyclo[2.2.2]octane units as a rigid spacer and as a carbocation precursor, 321
- Hydrogen peroxide
A SIFT study of the reactions of H_3O^+ , NO^+ and O_2^+ with hydrogen peroxide and peroxyacetic acid, 269
- Hydrogen transfer
The role of hydride migration in the mechanism of alcohol elimination from protonated ethers upon chemical ionization. Experiment and theory, 297
- Hydrogen-bridged radical cations
The remarkable decarbonylation of $\text{CH}_3\text{O-P-O}^+$ and its distonic isomer $\text{CH}_2\text{O-P-OH}^+$: an experimental and CBS-QB3 computational study, 759
- Inductively coupled plasma mass spectrometry
State-of-the-art in inorganic mass spectrometry for analysis of high-purity materials, 127
- Inelastic scattering
Surface-induced dissociation of acetone cations from self-assembled monolayer surface of fluorinated alkyl thiol on Au (1 1 1) substrate at low collision energies, 563
- Inorganic mass spectrometry
State-of-the-art in inorganic mass spectrometry for analysis of high-purity materials, 127
- Integral cross-sections
Reactions of molecular dications: collision energy dependence of integral cross-sections of processes in $\text{CHCl}_2^{2+} + \text{Ar}$, D_2 systems from guided beam studies, 487
- Interstellar chemistry
Optical detection of C_9H_3 , C_{11}H_3 , and C_{13}H_3 from a hydrocarbon discharge source, 647
- Ion clusters
Gas-phase ion chemistry in $\text{GeH}_4/\text{C}_2\text{H}_4/\text{XH}_3$ ($X = \text{P}, \text{N}$) systems, 403
- Ion fission
Collision-induced symmetric fission of doubly-charged cubelike $[\text{Fe}_4\text{S}_4\text{X}_4]^{2-}$ clusters, 797
- Ion implantation
Implanting atomic ions into surface adsorbed fullerenes: the single collision formation and emission of Cs@C_{60}^+ and Cs@C_{70}^+ , 1055
- Ion kinetic energy
Cross sections and ion kinetic energies for electron impact ionization of CH_4 , 307
- Ion mobility experiments
Distinguishing the topology of macrocyclic compounds and catenanes, 373
- Ion motion
Theory, simulation and measurement of chemical mass shifts in RF quadrupole ion traps, 237
- Ion parking
Ion/ion reactions of multiply charged nucleic acid anions: electron transfer, proton transfer, and ion attachment, 577
- Ion structures
The distinctive behavior of isomeric methyl ethyl mixed esters of 2-methylmaleic acid upon electron ionization, 191
- Ion trap mass spectrometry
Gas-phase ion chemistry in $\text{GeH}_4/\text{C}_2\text{H}_4/\text{XH}_3$ ($X = \text{P}, \text{N}$) systems, 403
- Ion/ion reactions
Ion/ion reactions of multiply charged nucleic acid anions: electron transfer, proton transfer, and ion attachment, 577
- Ion/molecule complexes
Proton-induced intra-complex hydride transfer involving bicyclo[2.2.2]octane units as a rigid spacer and as a carbocation precursor, 321
- Ion/molecule reaction
Reactions of 2-bromopropene radical cation with amines—a study by FT-ICR spectrometry and DFT calculation, 167
Atmospheric pressure photoionization mechanisms. 1. The case of acetonitrile, 841
- Ionisation
Intermediate species in a 2.45 GHz microwave plasma sustained in an argon–tetramethylsilane gas mixture, 49
- Ionization energy (IE)
FTICR-MS study of the gas-phase thermochemistry of americium oxides, 457
A theoretical study of the ground and excited states of the CHCl_2^{2+} dication and the CHCl^+ cation, 497
- Ion–molecule reactions
A SIFT study of the reactions of H_3O^+ , NO^+ and O_2^+ with hydrogen peroxide and peroxyacetic acid, 269
Internal energy effects in the reactivity of CO_2^{2+} doubly charged molecular ions with CO_2 and CO , 507
Hydrogen/deuterium exchange of electrosprayed ions in the atmospheric interface of a commercial triple–quadrupole mass spectrometer, 729
Reactions of gaseous halocarbonyl cations with aromatic compounds: ionic carbonylation of inert C–H bonds, 901
- Ion–neutral complex
Theoretical studies of methane elimination from C_4H_9^+ and H_2 elimination from C_3H_7^+ , 955
- Ion–surface collisions
Surface-induced dissociation of acetone cations from self-assembled monolayer surface of fluorinated alkyl thiol on Au (1 1 1) substrate at low collision energies, 563
- Iron–sulfur clusters
Collision-induced symmetric fission of doubly-charged cubelike $[\text{Fe}_4\text{S}_4\text{X}_4]^{2-}$ clusters, 797

- Isomer**
 Ab initio characterization of the weakly bound anions ClOO^- and ArCl^- , 667
- Isomerization**
 On the chemistry following methoxy migration in the metastably decomposing $(\text{M} - \text{COOCH}_3)^+$ ions (m/z 135) from dimethyl phthalate, isophthalate and terephthalate, 891
- Isotope ratio mass spectrometry**
 Stable isotope ratio mass spectrometry in global climate change research, 1
- Ketene**
 Catalytic gas phase dehydration of acetic acid to ketene, 599
- Kinetic energy release**
 How ergodic is the fragmentation of the pyridine cation? A maximum entropy analysis, 389
- Kinetic Energy Release Distribution (KERD)**
 Determining C_2 binding energies from KERDs for C_{80}^+ and C_{82}^+ fullerenes and their endohedrals, 181
- Kinetic method**
 Application of the kinetic method to bifunctional bases. ESI tandem quadrupole experiments, 1035
- Kinetics**
 Electron attachment and detachment: cyclo- $\text{C}_4\text{F}_4\text{Cl}_2$, 541
- Knots**
 Distinguishing the topology of macrocyclic compounds and catenanes, 373
- Knudsen-cell mass spectrometry**
 In situ synthesis and characterization of fullerene derivatives by Knudsen-cell mass spectrometry, 807
- La@C_{82}**
 Oxygen reactivity of La@C_{82} investigated with laser desorption mass spectrometry, 913
- LA-ICP-MS**
 Structural identification and quantification of protein phosphorylations after gel electrophoretic separation using Fourier transform ion cyclotron resonance mass spectrometry and laser ablation inductively coupled plasma mass spectrometry, 985
- Laser ablation**
 Production of small binary carbon clusters by laser ablation of thin films of derivatised fullerenes, 969
- Laser ablation ICP-MS**
 State-of-the-art in inorganic mass spectrometry for analysis of high-purity materials, 127
- Laser desorption mass spectrometry**
 Oxygen reactivity of La@C_{82} investigated with laser desorption mass spectrometry, 913
- LDI**
 The influence of phenylated by-products on the MALDI analysis of chlorinated fullerenes, 979
- Ligation**
 Investigations of the gas-phase reactivity of Cu^+ and Ag^+ glycine complexes towards CO, D_2O and NH_3 , 629
- Low-energy electrons**
 Formation of negative ions from gas phase halo-uracils by low-energy (0–18 eV) electron impact, 703
- Macrocycles**
 Distinguishing the topology of macrocyclic compounds and catenanes, 373
- Magic numbers**
 Determining C_2 binding energies from KERDs for C_{80}^+ and C_{82}^+ fullerenes and their endohedrals, 181
- MALDI**
 The influence of phenylated by-products on the MALDI analysis of chlorinated fullerenes, 979
- Mass spectra of isomers**
 The distinctive behavior of isomeric methyl ethyl mixed esters of 2-methylmaleic acid upon electron ionization, 191
- Mass spectrometry**
 Electrospray ionization and liquid secondary ion mass spectrometric study of N-heterocyclic carbenes and their 1,2,4-triazolium salt precursors, 61
 Gas-phase basicity and enantiodiscrimination of some phosphorous-containing α -amino acid mimics, 349
 Distinguishing the topology of macrocyclic compounds and catenanes, 373
 Structure, thermochemistry, and reactivity of MS_n^+ cations ($\text{M} = \text{V}, \text{Mo}$; $n = 1-3$) in the gas phase, 439
 Structures and fragmentations of electrosprayed Zn(II) complexes of carboxylic acids in the gas phase. Isomerisation versus desolvation during the last desolvation step, 779
- Mass spectrum**
 Field-induced ionization and Coulomb explosion of CO_2 by intense femtosecond laser pulses, 81
- MATI spectra**
 Enhancing of the signal-to-noise ratio in MATI spectra, 921
- Maximum entropy method**
 How ergodic is the fragmentation of the pyridine cation? A maximum entropy analysis, 389
- Mechanism of alcohol elimination**
 The role of hydride migration in the mechanism of alcohol elimination from protonated ethers upon chemical ionization. Experiment and theory, 297
- Mechanism of fragmentation**
 The distinctive behavior of isomeric methyl ethyl mixed esters of 2-methylmaleic acid upon electron ionization, 191
- Metal dications**
 Generation of “unstable” doubly charged metal ion complexes in a laser vaporization cluster source, 285
- Metal hydrocarbon compounds**
 Mass selective photodetachment photoelectron spectroscopy: small transition metal (Fe, Ni) carbon hydrogen compounds, 1067
- Metal ion solvation**
 Generation of “unstable” doubly charged metal ion complexes in a laser vaporization cluster source, 285
- Metal ions**
 Investigations of the gas-phase reactivity of Cu^+ and Ag^+ glycine complexes towards CO, D_2O and NH_3 , 629
- Metal salts**
 Investigations of the gas-phase reactivity of Cu^+ and Ag^+ glycine complexes towards CO, D_2O and NH_3 , 629

- Metal solvates**
Microsolvation of metal ions: on the stability of $[\text{Zr}(\text{CH}_3\text{CN})]^{4+}$ and other multiply charged ions, 517
- Metal sulfide cation**
Structure, thermochemistry, and reactivity of MS_n^+ cations ($\text{M} = \text{V}, \text{Mo}; n = 1-3$) in the gas phase, 439
- Metastable cluster ions**
Generation of "unstable" doubly charged metal ion complexes in a laser vaporization cluster source, 285
- Metastable ions**
Proton-induced intra-complex hydride transfer involving bicyclo[2.2.2]octane units as a rigid spacer and as a carbocation precursor, 321
Fragmentations of some dinitrile anions, 1083
- Methide abstraction**
Ligand exchange ion-molecule reactions of simple silyl and germyl cations, 551
- Methoxo-oxovanadium cluster**
Ion chemistry of the hexanuclear methoxo-oxovanadium cluster $\text{V}_6\text{O}_7(\text{OCH}_3)_{12}$, 743
- MIKE**
On the chemistry following methoxy migration in the metastably decomposing ($\text{M} - \text{COOCH}_3$) $^+$ ions (m/z 135) from dimethyl phthalate, isophthalate and terephthalate, 891
- MIKE-spectrometry**
Fragmentations of some dinitrile anions, 1083
- Molecular mousetraps**
Biomimetic approaches to gas phase peptide chemistry: combining selective binding motifs with reactive carbene precursors to form molecular mousetraps, 851
- Molecular orbital calculations**
Protonation and methylation of thiophenol, thioanisole and their halogenated derivatives: mass spectrometric and computational study, 151
- MS/MS**
Two-center three-electron bonds involving selenium, 429
Secondary fragmentation of linear peptides in electron capture dissociation, 723
- Multichannel RRKM**
Reactivity of gaseous protonated ozone: a computational investigation on the carbon monoxide oxidation reaction, 613
- Multiphoton absorption**
Enhancing of the signal-to-noise ratio in MATI spectra, 921
- Multiphoton ionization**
Enhancing of the signal-to-noise ratio in MATI spectra, 921
- Multiply charged ions**
Microsolvation of metal ions: on the stability of $[\text{Zr}(\text{CH}_3\text{CN})]^{4+}$ and other multiply charged ions, 517
- Multiply-charged anions**
Collision-induced symmetric fission of doubly-charged cubelike $[\text{Fe}_4\text{S}_4\text{X}_4]^{2-}$ clusters, 797
- Neutral fragment reionization**
Structural determinants for the evaporation of intact oligomers from collisionally activated cluster ions, 933
- Neutralization-reionization**
Neutralization-reionization of ions produced by electrospray. Instrument design and initial data, 687
- Neutrals**
Generation of neutrals from anionic precursors in the gas phase. The anionic, neutral and cationic rearrangements of CCCCHO and CCCHCO to HCCCCO, 467
- Nonlinear fields**
Theory, simulation and measurement of chemical mass shifts in RF quadrupole ion traps, 237
- Nucleophilic substitution**
Reactions of 2-bromopropene radical cation with amines—a study by FT-ICR spectrometry and DFT calculation, 167
- Oligonucleotide anions**
Ion/ion reactions of multiply charged nucleic acid anions: electron transfer, proton transfer, and ion attachment, 577
- Oxocarbon dianions**
Hydration of cyclic oxocarbon dianions, such as $\text{c-C}_5\text{O}_5^{2-}$, in the gas phase. Charge reduction of hydrates by electron detachment or proton transfer. Energy barriers for electron detachment and electron transfer, 1017
- Oxygen reactivity**
Oxygen reactivity of La@C_{82} investigated with laser desorption mass spectrometry, 913
- Ozonation**
The impervious route to the elusive HOOO^- anion, 717
- Ozone chemistry**
Reactivity of gaseous protonated ozone: a computational investigation on the carbon monoxide oxidation reaction, 613
- Pentaquadrupole mass spectrometry**
Reactions of gaseous halocarbonyl cations with aromatic compounds: ionic carbonylation of inert C-H bonds, 901
- Peptide-protein interaction**
Tandem mass spectrometric characterization of branched peptides derived from photoaffinity labeling, 527
- Peptides**
Biomimetic approaches to gas phase peptide chemistry: combining selective binding motifs with reactive carbene precursors to form molecular mousetraps, 851
- Peptidomimetics**
Structural analysis of high affinity divalent phosphopeptide hybrids of spleen tyrosine kinase, 879
- Peroxyacetic acid**
A SIFT study of the reactions of H_3O^+ , NO^+ and O_2^+ with hydrogen peroxide and peroxyacetic acid, 269
- Phase space**
How ergodic is the fragmentation of the pyridine cation? A maximum entropy analysis, 389
- Phosphine**
Gas-phase ion chemistry in $\text{GeH}_4/\text{C}_2\text{H}_4/\text{XH}_3$ ($\text{X} = \text{P}, \text{N}$) systems, 403
- O-Phospho α -amino acids**
Gas-phase basicity and enantiodiscrimination of some phosphorous-containing α -amino acid mimics, 349

- Phosphorus**
Structural identification and quantification of protein phosphorylations after gel electrophoretic separation using Fourier transform ion cyclotron resonance mass spectrometry and laser ablation inductively coupled plasma mass spectrometry, 985
- Phosphorylation**
Structural analysis of high affinity divalent phosphopeptide hybrids of spleen tyrosine kinase, 879
- Photodetachment**
Mass selective photodetachment photoelectron spectroscopy: small transition metal (Fe, Ni) carbon hydrogen compounds, 1067
- Photodissociation**
Generation of “unstable” doubly charged metal ion complexes in a laser vaporization cluster source, 285
Ultrafast dynamics of acetone–water clusters: the influence of solvation, 677
- Photoelectron spectra**
Mass selective photodetachment photoelectron spectroscopy: small transition metal (Fe, Ni) carbon hydrogen compounds, 1067
- Photoionization**
Internal energy effects in the reactivity of CO_2^{2+} doubly charged molecular ions with CO_2 and CO , 507
Atmospheric pressure photoionization mechanisms. 1. The case of acetonitrile, 841
- Plasma**
Intermediate species in a 2.45 GHz microwave plasma sustained in an argon–tetramethylsilane gas mixture, 49
- Plutonium oxide**
FTICR-MS study of the gas-phase thermochemistry of americium oxides, 457
- Primary amine**
Biomimetic approaches to gas phase peptide chemistry: combining selective binding motifs with reactive carbene precursors to form molecular mousetraps, 851
- Product ion spectra**
ESI/MS/MS in characterization of diastereomeric intermediates in the stereocontrolled synthesis of protoberberines, 209
- Proteins**
Structural identification and quantification of protein phosphorylations after gel electrophoretic separation using Fourier transform ion cyclotron resonance mass spectrometry and laser ablation inductively coupled plasma mass spectrometry, 985
- Proton affinity**
A comprehensive computational investigation of the enthalpies of formation and proton affinities of $\text{C}_4\text{H}_7\text{N}$ and $\text{C}_3\text{H}_3\text{ON}$ compounds, 91
Gas-phase basicity and enantiodiscrimination of some phosphorous-containing α -amino acid mimics, 349
Application of the kinetic method to bifunctional bases. ESI tandem quadrupole experiments, 1035
- Proton and methyl cation affinities**
Protonation and methylation of thiophenol, thioanisole and their halogenated derivatives: mass spectrometric and computational study, 151
- Proton transfer**
Selected ion flow tube, SIFT, studies of the reactions of H_3O^+ , NO^+ and O_2^+ with eleven $\text{C}_{10}\text{H}_{16}$ monoterpenes, 117
Proton-induced intra-complex hydride transfer involving bicyclo[2.2.2]octane units as a rigid spacer and as a carbocation precursor, 321
Reactions of molecular dications: collision energy dependence of integral cross-sections of processes in $\text{CHCl}_2^{2+} + \text{Ar}$, D_2 systems from guided beam studies, 487
- Protonation**
Atmospheric pressure photoionization mechanisms. 1. The case of acetonitrile, 841
- Protonation entropy**
Application of the kinetic method to bifunctional bases. ESI tandem quadrupole experiments, 1035
- Protonolysis**
Proton-induced intra-complex hydride transfer involving bicyclo[2.2.2]octane units as a rigid spacer and as a carbocation precursor, 321
- Proton-transport catalysis**
The remarkable decarbonylation of $\text{CH}_3\text{O}-\text{P}=\text{O}^{*+}$ and its distonic isomer $\text{CH}_2\text{O}-\text{P}-\text{OH}^{*+}$: an experimental and CBS-QB3 computational study, 759
- Pyridine ion**
How ergodic is the fragmentation of the pyridine cation?. A maximum entropy analysis, 389
- Quantum calculations**
Structures and fragmentations of electrosprayed Zn(II) complexes of carboxylic acids in the gas phase. Isomerisation versus desolvation during the last desolvation step, 779
- Quantum chemistry**
Fragmentations of some dinitrile anions, 1083
- Reaction mechanism**
Reactions of 2-bromopropene radical cation with amines—a study by FT-ICR spectrometry and DFT calculation, 167
Reactivity of gaseous protonated ozone: a computational investigation on the carbon monoxide oxidation reaction, 613
Fragmentations of some dinitrile anions, 1083
- Resonances**
Formation of negative ions from gas phase halo-uracils by low-energy (0–18 eV) electron impact, 703
- RF quadrupole ion trap**
Theory, simulation and measurement of chemical mass shifts in RF quadrupole ion traps, 237
- Salt bridges**
Structural determinants for the evaporation of intact oligomers from collisionally activated cluster ions, 933
- Secondary fragmentation**
Secondary fragmentation of linear peptides in electron capture dissociation, 723
- Selenium**
Two-center three-electron bonds involving selenium, 429

SH2 domains

Structural analysis of high affinity divalent phosphopeptide hybrids of spleen tyrosine kinase, 879

SIFT

Selected ion flow tube, SIFT, studies of the reactions of H_3O^+ , NO^+ and O_2^+ with eleven $\text{C}_{10}\text{H}_{16}$ monoterpenes, 117

A SIFT study of the reactions of H_3O^+ , NO^+ and O_2^+ with hydrogen peroxide and peroxyacetic acid, 269

SIFT-MS

Selected ion flow tube, SIFT, studies of the reactions of H_3O^+ , NO^+ and O_2^+ with eleven $\text{C}_{10}\text{H}_{16}$ monoterpenes, 117

Quantification of acetonitrile in exhaled breath and urinary headspace using selected ion flow tube mass spectrometry, 655

Signal-to-noise ratio

Enhancing of the signal-to-noise ratio in MATI spectra, 921

Silver ions

Sequential bond energies of $\text{Ag}^+(\text{H}_2\text{O})_n$ and $\text{Ag}^+(\text{dimethyl ether})_n$, $n = 1-4$, determined by threshold collision-induced dissociation, 221

Silyl and germyl migration

Ligand exchange ion-molecule reactions of simple silyl and germyl cations, 551

Silyl ions

Ligand exchange ion-molecule reactions of simple silyl and germyl cations, 551

Simulation

Theory, simulation and measurement of chemical mass shifts in RF quadrupole ion traps, 237

Skeletal rearrangement

Proton-induced intra-complex hydride transfer involving bicyclo[2.2.2]octane units as a rigid spacer and as a carbocation precursor, 321

Small binary carbon clusters

Production of small binary carbon clusters by laser ablation of thin films of derivatised fullerenes, 969

Smoking

Quantification of acetonitrile in exhaled breath and urinary headspace using selected ion flow tube mass spectrometry, 655

Sodium ion affinity

Na^+ affinities of gas-phase amino acids by ligand exchange equilibrium, 825

Solvation

Sequential bond energies of $\text{Ag}^+(\text{H}_2\text{O})_n$ and $\text{Ag}^+(\text{dimethyl ether})_n$, $n = 1-4$, determined by threshold collision-induced dissociation, 221

Solvation effects

Ultrafast dynamics of acetone-water clusters: the influence of solvation, 677

Specific reactivity

Specific reactivity of 1-alkenes with transition metal cations. 1-Pentene- and 1-octene- Cu^+ reactions in the gas phase, 359

Stable isotopes

Stable isotope ratio mass spectrometry in global climate change research, 1

Statistical theory

How ergodic is the fragmentation of the pyridine cation? A maximum entropy analysis, 389

Stereospecific fragmentation

The role of hydride migration in the mechanism of alcohol elimination from protonated ethers upon chemical ionization. Experiment and theory, 297

Supramolecular chemistry

Distinguishing the topology of macrocyclic compounds and catenanes, 373

Surface scattering

Implanting atomic ions into surface adsorbed fullerenes: the single collision formation and emission of Cs@C_{60}^+ and Cs@C_{70}^+ , 1055

Surface-induced dissociation

Surface-induced dissociation of acetone cations from self-assembled monolayer surface of fluorinated alkyl thiol on Au (1 1 1) substrate at low collision energies, 563

Syk inhibitors

Structural analysis of high affinity divalent phosphopeptide hybrids of spleen tyrosine kinase, 879

Tandem mass spectrometry

Catalytic gas phase dehydration of acetic acid to ketene, 599

Tandem MS

Secondary fragmentation of linear peptides in electron capture dissociation, 723

Terpenes

Selected ion flow tube, SIFT, studies of the reactions of H_3O^+ , NO^+ and O_2^+ with eleven $\text{C}_{10}\text{H}_{16}$ monoterpenes, 117

tert-Butylbenzenes

Proton-induced intra-complex hydride transfer involving bicyclo[2.2.2]octane units as a rigid spacer and as a carbocation precursor, 321

Tetramethylsilane

Intermediate species in a 2.45 GHz microwave plasma sustained in an argon-tetramethylsilane gas mixture, 49

Thermochemistry

Sequential bond energies of $\text{Ag}^+(\text{H}_2\text{O})_n$ and $\text{Ag}^+(\text{dimethyl ether})_n$, $n = 1-4$, determined by threshold collision-induced dissociation, 221

Structure, thermochemistry, and reactivity of MS_n^+ cations ($\text{M} = \text{V}, \text{Mo}$; $n = 1-3$) in the gas phase, 439

FTICR-MS study of the gas-phase thermochemistry of americium oxides, 457

Ab initio characterization of the weakly bound anions ClOO^- and ArCl^- , 667

Thiophenols

Protonation and methylation of thiophenol, thioanisole and their halogenated derivatives: mass spectrometric and computational study, 151

Threshold ionisation

Intermediate species in a 2.45 GHz microwave plasma sustained in an argon-tetramethylsilane gas mixture, 49

Trace analysis

State-of-the-art in inorganic mass spectrometry for analysis of high-purity materials, 127

Transition metal

Specific reactivity of 1-alkenes with transition metal cations. 1-Pentene- and 1-octene- Cu^+ reactions in the gas phase, 359

Transition metal fluorides

In situ synthesis and characterization of fullerene derivatives by Knudsen-cell mass spectrometry, 807

Translational energy release

Theoretical studies of methane elimination from $C_4H_9^+$ and H_2 elimination from $C_3H_7^+$, 955

Trapping by proxy

Ion/ion reactions of multiply charged nucleic acid anions: electron transfer, proton transfer, and ion attachment, 577

Triazolium salts

Electrospray ionization and liquid secondary ion mass spectrometric study of N-heterocyclic carbenes and their 1,2,4-triazolium salt precursors, 61

Trifluoromethylation

In situ synthesis and characterization of fullerene derivatives by Knudsen-cell mass spectrometry, 807

Tropospheric chemistry

A comprehensive computational investigation of the enthalpies of formation and proton affinities of C_4H_7N and C_3H_3ON compounds, 91

Tropospheric pollution

The impervious route to the elusive HO_3^- anion, 717

Urine

Quantification of acetonitrile in exhaled breath and urinary headspace using selected ion flow tube mass spectrometry, 655

Vacuum ultraviolet

Internal energy effects in the reactivity of CO_2^{2+} doubly charged molecular ions with CO_2 and CO , 507

van der Waals

Ab initio characterization of the weakly bound anions $ClOO^-$ and $ArCl^-$, 667

Vanadium oxides

Ion chemistry of the hexanuclear methoxo-oxovanadium cluster $V_6O_7(OCH_3)_{12}$, 743

Water

Sequential bond energies of $Ag^+(H_2O)_n$ and $Ag^+(\text{dimethyl ether})_n$, $n = 1-4$, determined by threshold collision-induced dissociation, 221

Woodward-Hoffmann

Theoretical studies of methane elimination from $C_4H_9^+$ and H_2 elimination from $C_3H_7^+$, 955

p-Xylene

Enhancing of the signal-to-noise ratio in MATI spectra, 921

Zinc binding

Zinc binding properties of the amyloid fragment $A\beta(1-16)$ studied by electrospray-ionization mass spectrometry, 999

Zinc complexes

Structures and fragmentations of electrosprayed $Zn(II)$ complexes of carboxylic acids in the gas phase. Isomerisation versus desolvation during the last desolvation step, 779